US Army Corps of Engineers

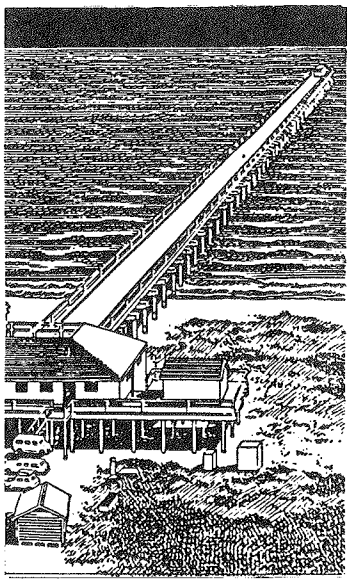

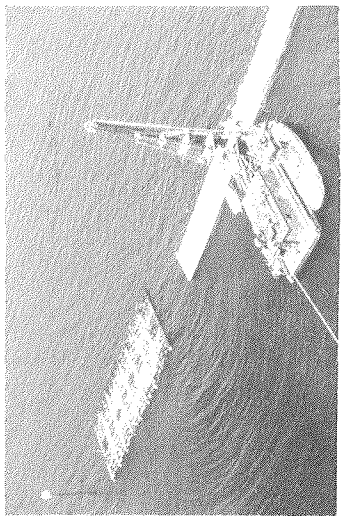

COASTAL ENGINEERING RESEARCH CENTER

MISCELLANEOUS PAPER CERC-89-1

FLOATING BREAKWATER PROTOTYPE TEST PROGRAM: SUMMARY OF DATA ANALYSIS EFFORTS

by

Peter J. Grace, Paul F. Mlakar

Coastal Engineering Research Center

DEPARTMENT OF THE ARMY
Waterways Experiment Station, Corps of Engineers
PO Box 631, Vicksburg, Mississippi 39181-0631

US ARMY ENGINEER WATERWAYS EXPERIMENT STATION

January 1989
Final Report

Prepared for DEPARTMENT OF THE ARMY
US Army Corps of Engineers
Washington, DC 20314-1000

Under Coastal Structures Evaluation
and Design Work Unit 31679

Destroy this report when no longer needed. Do not return it to the originator.

The findings in this report are not to be construed as an official Department of the Army position unless so designated by other authorized documents.

The contents of this report are not to be used for advertising, publication, or promotional purposes. Citation of trade names does not constitute an official endorsement or approval of the use of such commercial products.

Unclassified
SECURITY CLASSIFICATION OF THIS PAGE

REPORT DOCUMENTATION PAGE

Form Approved
OMB No 0704-0188
Exp. Date Jun 30, 1986

1a. REPORT SECURITY CLASSIFICATION
Unclassified

1b. RESTRICTIVE MARKINGS

2a. SECURITY CLASSIFICATION AUTHORITY

2b. DECLASSIFICATION / DOWNGRADING SCHEDULE

3. DISTRIBUTION / AVAILABILITY OF REPORT
Approved for public release; distribution unlimited.

4. PERFORMING ORGANIZATION REPORT NUMBER(S)
Miscellaneous Paper CERC-89-1

5. MONITORING ORGANIZATION REPORT NUMBER(S)

6a. NAME OF PERFORMING ORGANIZATION
USAEWES, Coastal Engineering Research Center

6b. OFFICE SYMBOL (If applicable)

7a. NAME OF MONITORING ORGANIZATION

6c. ADDRESS (City, State, and ZIP Code)
PO Box 631
Vicksburg, MS 39181-0631

7b. ADDRESS (City, State, and ZIP Code)

8a. NAME OF FUNDING / SPONSORING ORGANIZATION
US Army Corps of Engineers

8b. OFFICE SYMBOL (If applicable)

9. PROCUREMENT INSTRUMENT IDENTIFICATION NUMBER

8c. ADDRESS (City, State, and ZIP Code)
Washington, DC 20314-1000

10. SOURCE OF FUNDING NUMBERS

PROGRAM ELEMENT NO.	PROJECT NO.	TASK NO.	WORK UNIT ACCESSION NO
			31679

11. TITLE (Include Security Classification)
Floating Breakwater Prototype Test Program: Summary of Data Analysis Efforts

12. PERSONAL AUTHOR(S)
Grace, Peter J., Mlakar, Paul F.

13a. TYPE OF REPORT	13b. TIME COVERED	14. DATE OF REPORT (Year, Month, Day)	15. PAGE COUNT
Final report	FROM _____ TO _____	January 1989	38

16. SUPPLEMENTARY NOTATION
Available from National Technical Information Service, 5285 Port Royal Road, Springfield, VA 22161.

17. COSATI CODES			18. SUBJECT TERMS (Continue on reverse if necessary and identify by block number)
FIELD	GROUP	SUB-GROUP	Floating breakwater Hydrodynamics Structural response

19. ABSTRACT (Continue on reverse if necessary and identify by block number)

The Floating Breakwater Prototype Test Program (FBPTP) was initiated in 1981 in an effort to develop design criteria for floating breakwater applications in lakes, reservoirs, and semi-protected coastal waters. Some of the objectives of the program were to (a) determine the most effective breakwater design for a given wave climate; (b) establish the forces and moments which act on floating structures and their anchoring systems; and (c) determine loads on connecting mechanisms between individual breakwater modules. This paper describes analysis techniques used to reduce prototype data related to the above objectives.

20. DISTRIBUTION / AVAILABILITY OF ABSTRACT
☒ UNCLASSIFIED/UNLIMITED ☐ SAME AS RPT. ☐ DTIC USERS

21. ABSTRACT SECURITY CLASSIFICATION
Unclassified

22a. NAME OF RESPONSIBLE INDIVIDUAL

22b. TELEPHONE (Include Area Code)

22c. OFFICE SYMBOL

DD FORM 1473, 84 MAR

83 APR edition may be used until exhausted.
All other editions are obsolete.

SECURITY CLASSIFICATION OF THIS PAGE
Unclassified

PREFACE

This report documents the results of efforts to analyze data collected during a previously completed prototype monitoring investigation. The work was sponsored through funds provided to the Coastal Engineering Research Center (CERC) of the US Army Engineer Waterways Experiment Station (WES) by the Civil Works Directorate, US Army Corps of Engineers (USACE) under Coastal Structures Evaluation and Design Work Unit 31679, "Design of Floating Breakwaters." USACE point of contact was Mr. Jesse Pfeiffer, Jr., and USACE Technical Monitors were Messrs. John H. Lockhart, Jr., John G. Housley, Charles W. Hummer, and James E. Crews. Dr. C. Linwood Vincent is CERC's Program Manager.

These analysis efforts were coordinated by Mr. Peter J. Grace, Research Hydraulic Engineer, Wave Dynamics Division, CERC, under general supervision of Dr. James R. Houston and Mr. Charles C. Calhoun, Jr., Chief and Assistant Chief, CERC, respectively; and under direct supervision of Mr. C. Eugene Chatham, Jr., Chief, Wave Dynamics Division, and Mr. D. D. Davidson, Chief, Wave Research Branch. This report was prepared by Mr. Grace and Dr. Paul F. Mlakar, Chief Engineer, Structures Division, Jaycor, Inc.

Commander and Director of WES during publication of this report was COL Dwayne G. Lee, EN. Technical Director was Dr. Robert W. Whalin.

CONTENTS

CONVERSION FACTORS, NON-SI TO SI (METRIC) UNITS OF MEASUREMENT

Non-SI units of measurement used in this report can be converted to SI (metric) units as follows:

Multiply	By	To Obtain
cubic feet	Ø.Ø2831685	cubic meters
feet	Ø.3Ø48	meters
inches	2.54	centimeters
kips (force)	4.448222	kilonewtons
pounds (force)	4.448222	newtons
square feet	Ø.Ø929Ø3Ø4	square meters
tons (2,ØØØ pounds, mass)	9Ø7.1847	kilograms

FLOATING BREAKWATER PROTOTYPE TEST PROGRAM
SUMMARY OF DATA ANALYSIS EFFORTS

PART I: INTRODUCTION

1. The Floating Breakwater Prototype Test Program (FBPTP) was initiated in 1981 in an effort to develop design criteria for floating breakwater applications in lakes, reservoirs, and semi-protected coastal waters. The project involved investigations of design, construction, performance, and maintenance of a pipe-tire floating breakwater and a concrete structure (Nelson and Broderick, 1986). Actual data collection was accomplished between August 1982 and January 1984.

2. The monitoring system, which included the data acquisition system and all corresponding instrumentation, was designed and operated by the Civil Engineering Department of the University of Washington (Christensen, 1984). A total of 78 data measuring devices was located on or near the two floating breakwaters. Environmental data which were collected included wind speed and direction, current velocity, and water and air temperatures. Incident and transmitted wave heights were measured using a pile mounted staff gage and four spar buoys. Between October 1983 and January 1984, directional wave information was recorded using an eight-gage linear wave buoy array. Anchor line forces were measured on both the pipe-tire and concrete breakwaters. Additional instrumentation of the concrete breakwater included side- and bottom-mounted pressure transducers, linear and angular accelerometers, relative motion sensors, and internal strain gages mounted on portions of the concrete reinforcing steel. Connector forces between adjacent breakwater modules also were measured successfully during latter stages

of the monitoring effort.

3. During this project, data were collected using 8.5-minute time series and a sampling rate of 4.Ø hertz; therefore, each time series contained approximately 2Ø48 samples of data. These data records were first reduced by means of a statistical analysis which provided the maximum, minimum, and mean values from each time series. The standard deviation of each record was also calculated. It was assumed that wave heights, and those parameters measured in response to the waves, were Rayleigh distributed. This allowed calculations of the significant and peak values based on the following relationships inherent to the Rayleigh distribution assumption:

$$\begin{aligned} \underline{X}s \cong Xmo &= 4\sigma \\ \bar{X} &= \emptyset.63(Xs) = 2.51\sigma \\ X_{10} &= 1.27(Xs) = 5.\emptyset8\sigma \\ \text{and } X_{1} &= 1.67(Xs) = 6.68\sigma \end{aligned}$$

where: Xs is the significant value; Xmo is the zero moment value (significant value based on the energy spectrum); σ is the standard deviation; $\bar{X}$ is the mean value; X_{10} is the average of the highest 1Ø percent of all values; and X_1 is the average of the highest 1 percent of all values. The Rayleigh distribution assumption was checked for validity by examining various records of wave height, anchor force, strain, pressure, and acceleration data. Spectral analysis techniques were also used to identify the important frequencies represented in each time series. These techniques allowed estimates of the energy spectra (distributions of energy as a function of frequency). Energy spectra were calculated using the fast fourier transform (FFT) algorithm. These spectra yielded the particular frequencies which corresponded to the highest levels of energy density. As expected, results showed that the peak energy frequency of the incident wave field was an important para-

meter to consider because the peak energy frequencies of other data such as anchor forces and internal strains often corresponded to that peak wave frequency. When the frequencies did not correspond, they typically were shifted by one spectral bandwidth which could have been a function of the averaging done when calculating the FFT. Peak values of the anchor force data were of primary interest; however, since these data were filtered to remove high frequency noise, the peak values were not valid. For this reason, the statistical value of the highest one percent of the readings within a time series was used to represent the peak force. The data analysis software developed by the University of Washington included methods for computing the cross-spectral phase and coherency between two channels. This particular analysis tool was used extensively, especially in the reduction of the strain and pressure data. The periodicity within time series was identified and checked using coherency methods which essentially expressed the ratio of spectral energy density of the two channels in question. Under ideal contions where there were no energy losses in transfer between channels, and no contaminating noise, a coherency of unity would be achieved. The phase angle allowed a comparison of different data channels based on the spectral lag in angle separation between the two channels. Values of Ø degrees and 18Ø degrees indicated channels which were perfectly in phase and out of phase, respectively. In addition to identifying dominant frequencies as mentioned above, these spectral analysis methods were also used to check for proper functional behavior of the strain, pressure, and wave gages, and in attempts to determine effective wave crest lengths.

PART II: PIPE-TIRE BREAKWATER RESULTS

Mooring Forces

4. The anchor line force data resulting from monitoring of the pipe-tire breakwater is presented graphically in Figures 1 and 2, as related to wave height and wave period, respectively. These figures indicate that the expected increase in anchor line force did not occur as the incident wave height and/or period increased. Measured anchor line forces were nearly constant at approximately 75 pounds per linear foot of breakwater regardless of wave height or period. These results do not compare well with corresponding results from previous model studies, even those studies conducted at prototype scale. The most probable cause of this discrepancy is related to the difference in materials used for the mooring lines, and the fact that model tests were performed in two-dimensional flumes with monochromatic waves. The prototype breakwater utilized nylon rope mooring lines which were more compliant than those anchoring systems used in previous laboratory investigations.

5. A similar prototype study was conducted by the Canadian National Water Research Institute at a small marina in Burlington, Ontario in 1981 and 1982 (Bishop 1984). The breakwater tested there was a Goodyear design and moorings consisted of steel chains connected to concrete gravity anchors; therefore, these moorings also lacked the elastic properties of the FBPTP anchoring system. The gages at the Canadian marina were in place for approximately five months and the largest loads encountered were 1,214 lb. on a center line and 1,417 lb. on a corner line. These loads were induced by storm generated waves

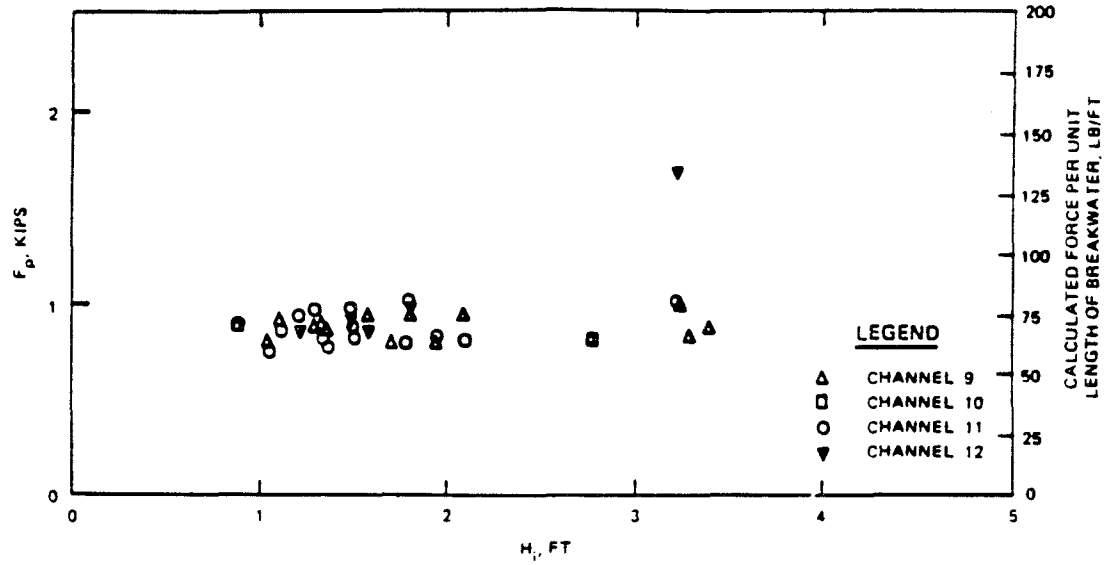

Figure 1. Peak anchor line force, Fp, versus incident wave height, Hi; pipe-tire breakwater

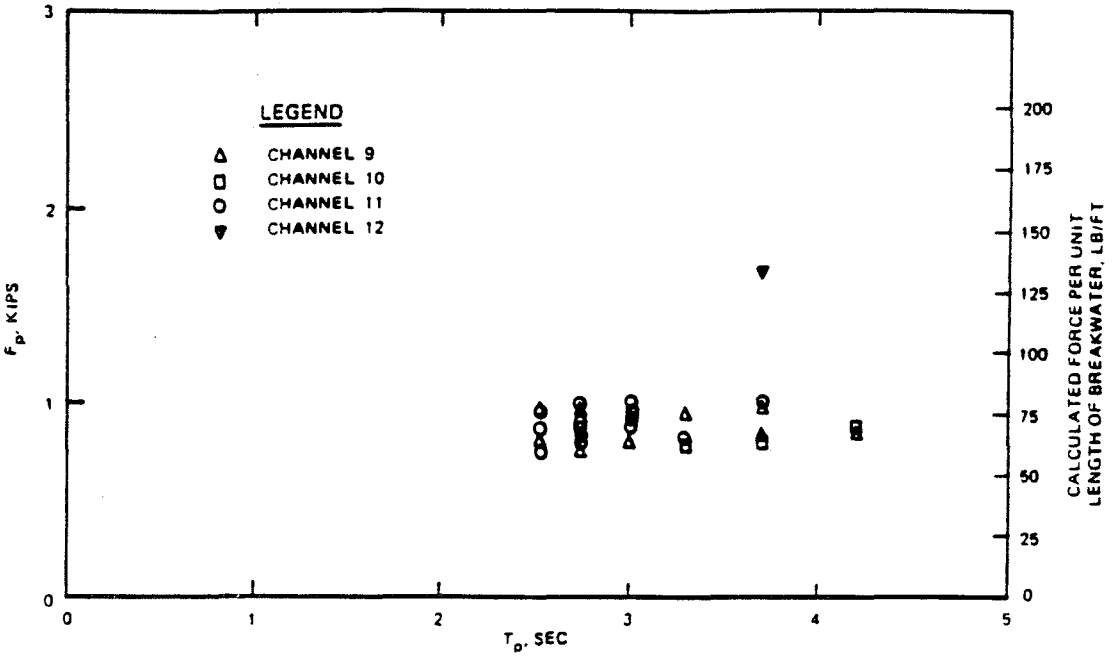

Figure 2. Peak anchor line force, Fp, versus wave period; pipe-tire breakwater

with heights estimated at about 2.1 feet. The maximum loads were approximately equivilant to 8Ø pounds per linear foot of breakwater, which corresponds well to the FBPTP measurements; however, the Canadian results did indicate an increase in mooring force magnitude with increasing wave heights and periods.

6. In 1985, a Goodyear floating tire breakwater in shallow water was monitored in similar fashion at Pickering Beach, Delaware (Grace and Clausner, 1987); however, this study involved subjection of the breakwater only to ship generated waves. Numerous test runs involving various boat speeds, sailing lines, and angles of wave approach revealed that the wake generating vessel produced a maximum wake height of 1.6 feet at full throttle (26 knots) while passing 75 feet from the breakwater. This resulted in a peak mooring line load of 281 lb. Mooring lines at this site consisted of polyester rope with a breaking strength of 19,4ØØ lb. The working load was 2,13Ø lb. (11 percent of the breaking strength); therefore, forces of similar magnitude to the boat wake induced forces recorded in this study should have no effect on the integrity of the mooring system.

Wave Attenuation

7. The wave-attenuating performance of the pipe-tire breakwater is presented in Figures 3 and 4, as related to wave height and period, respectively. Reliable wave transmission data were collected with incident wave heights ranging from 1.Ø to 2.4 feet and periods of 2 to 4 seconds. The breakwater achieved a transmission coefficient of approximately Ø.42 for incident waves up to about 2 feet in height. Figure 4 indicates that the transmission coefficient increased with correspond-

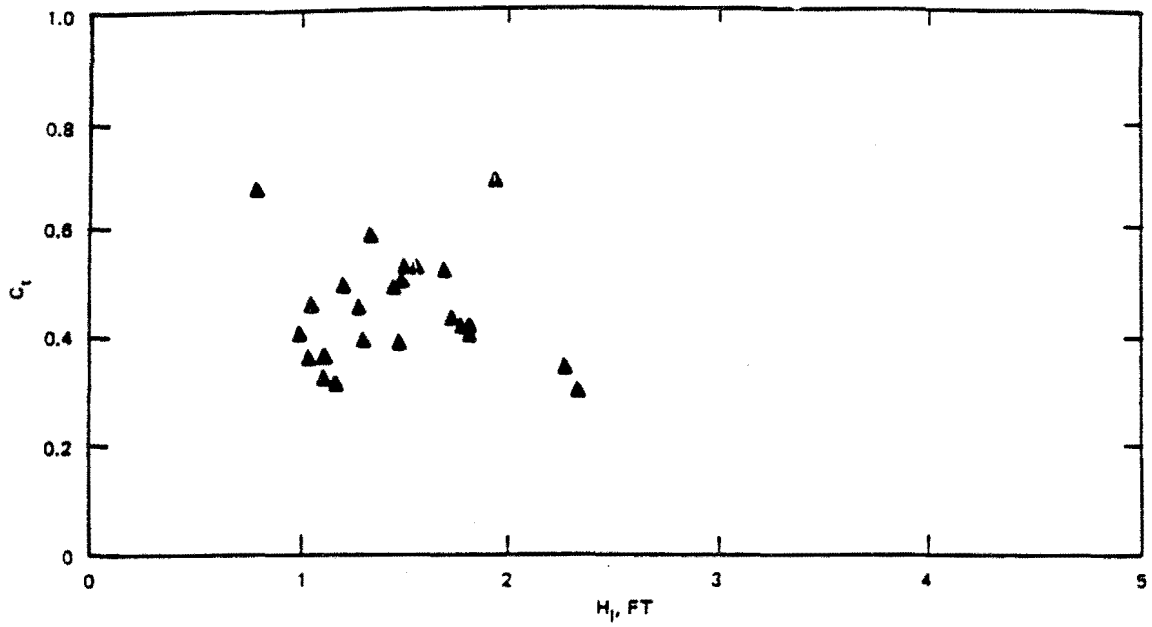

Figure 3. Transmission coefficient, Ct, versus incident wave height, Hi; pipe-tire breakwater

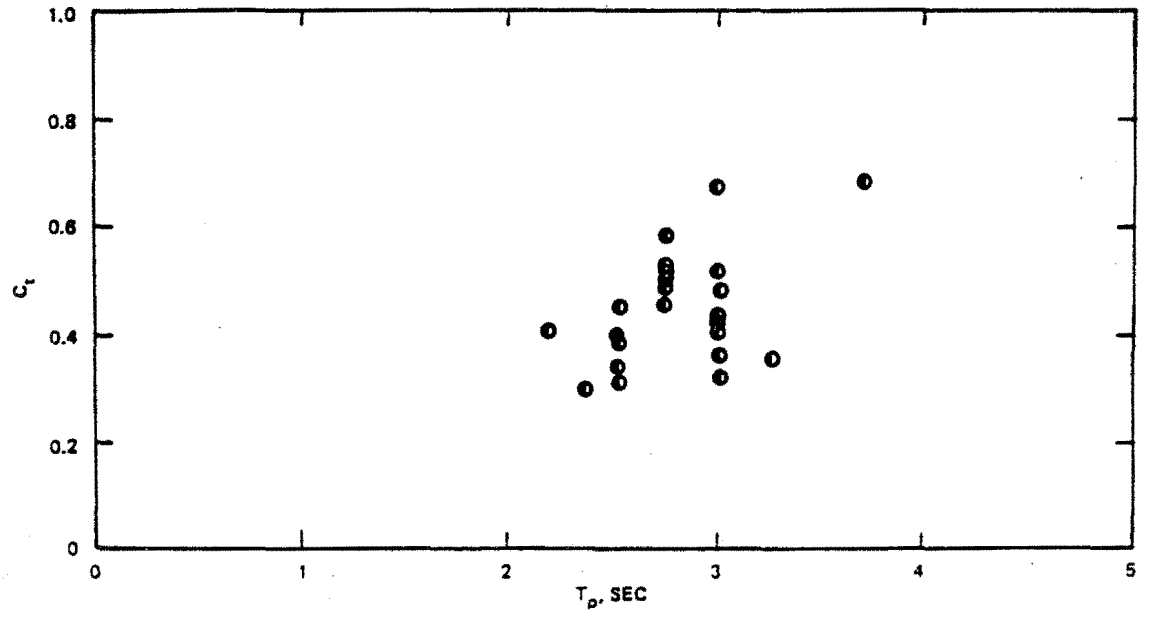

Figure 4. Transmission coefficient, Ct, versus wave period; pipe-tire breakwater

ing increasing wave periods; however, the range of wave periods experienced at the site was not sufficient to establish a conclusive trend.

PART III: CONCRETE BREAKWATER RESULTS

Mooring Forces

8. The two unit modular design of the concrete breakwater allowed testing of several various breakwater configurations which differed depending on the method used to connect the two breakwater sections. Monitoring also was conducted with and without clump weights attached to the anchor lines to evaluate their effect on breakwater performance and response. Successful data acquisition was accomplished for the four configurations listed below:

a. Rigid connection, with clump weights
b. Rigid connection, without clump weights
c. Vertical flexible connection, without clump weights
and d. Horizontal flexible connection, without clump weights.

9. Reliable anchor line force data were collected on channels 4 and 7, which represent the upper and lower load cells, respectively, on the southwestern-most anchor line. This data is presented in Figures 5-8. Figures 5 and 6 are plots of the peak anchor line force measured in one anchor line versus incident wave height. Figures 7 and 8 present the peak mooring line force versus wave period. The figures do not indicate a strong dependence of anchor line forces on the incident wave heights or periods as would normally be expected. Peak forces did increase slightly with increasing wave heights; however, these forces were much smaller than the predicted forces. Measured values averaged approximately 40 pounds per linear foot of breakwater. It should be noted that the measured force was that force above the initial anchor line tension which was approximately 133 lb/ft with clump weights and 40 lb/ft without clump weights. The figures also indicate that forces

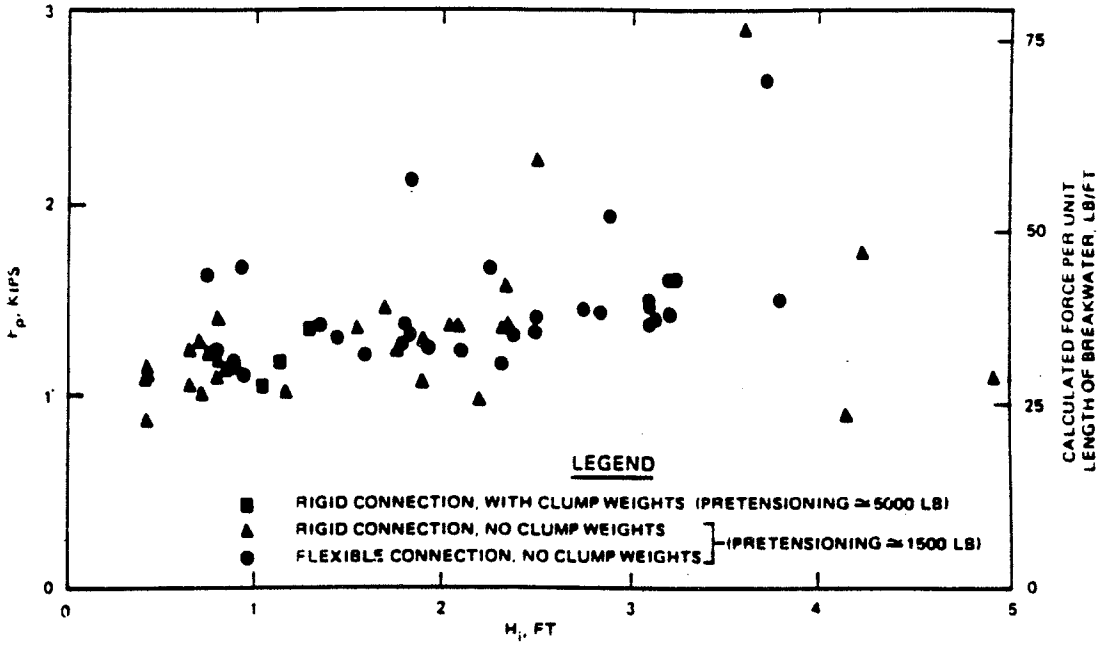

Figure 5. Peak anchor line force, Fp, versus incident wave height, Hi; concrete breakwater (channel 4)

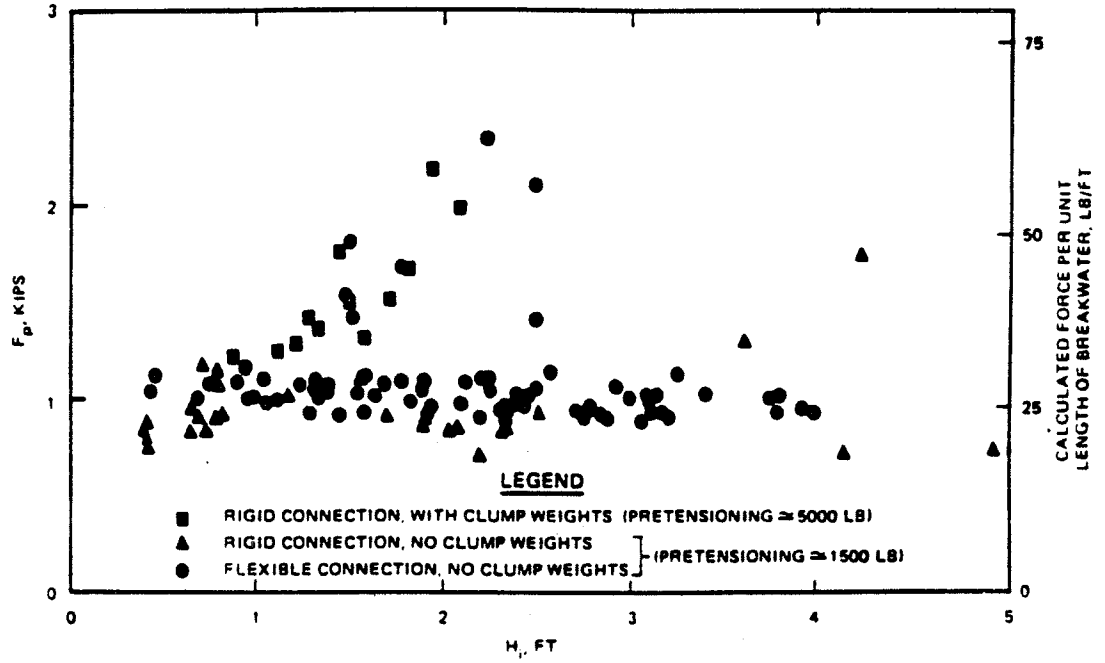

Figure 6. Peak anchor line force, Fp, versus incident wave height, Hi; concrete breakwater (channel 7)

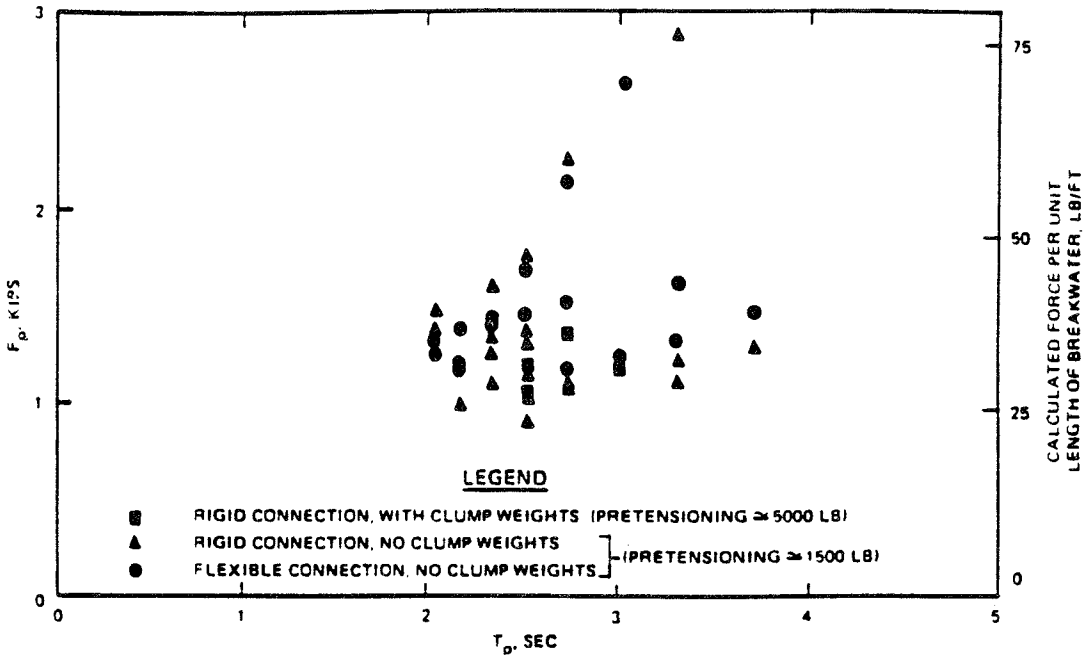

Figure 7. Peak anchor line force, Fp, versus wave period, Tp; concrete breakwater (channel 4)

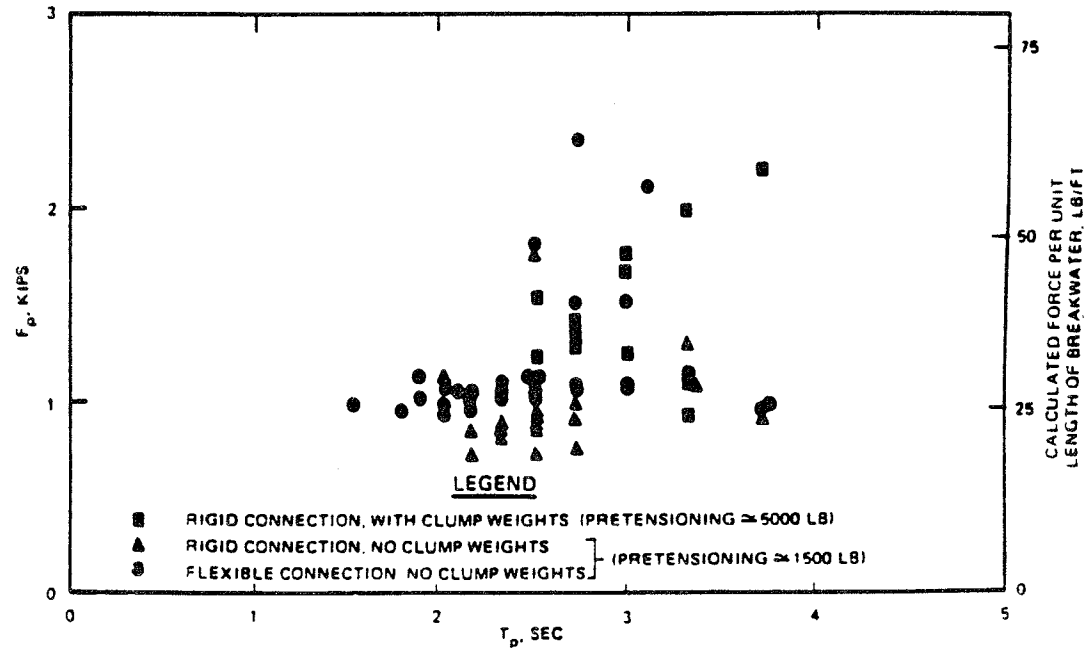

Figure 8. Peak anchor line force, Fp, versus wave period, Tp; concrete breakwater (channel 7)

in the upper load cell were slightly greater (about 25%) than the corresponding forces in the lower load cell. Clump weight removal resulted in an increase in the upper anchor line load while loads in the lower load cell decreased. Differences in the module connecting mechanisms demonstrated no substantial effect on the mooring line forces.

Wave Attenuation

10. Wave transmission data indicated that the concrete breakwater provided adequate protection for incident wave heights up to about 3 feet and periods up to 4 seconds. A transmission coefficient which centered around a value of Ø.4Ø was achieved with little dependence on wave height or period. This is demonstrated in Figure 9, a plot of transmission coefficient versus incident wave height. Ordinarily, the wave attenuating ability is expected to decrease significantly with increasing wave periods. Unfortunately, the range of wave periods experienced at the test site was limited as shown in Figure 1Ø, a plot of transmission coefficient versus wave period. As a result, no definate conclusions could be made relative to wave period effects. As was previously demonstrated with the mooring line forces, the module connecting method had no significant effect on the breakwater's wave attenuating ability.

Hydrodynamic Pressures

11. Prior to 1985, most data reduction efforts had been directed at analysis of wave characteristics and mooring line forces. More recently, greater emphasis has been placed on the analysis and interpre-

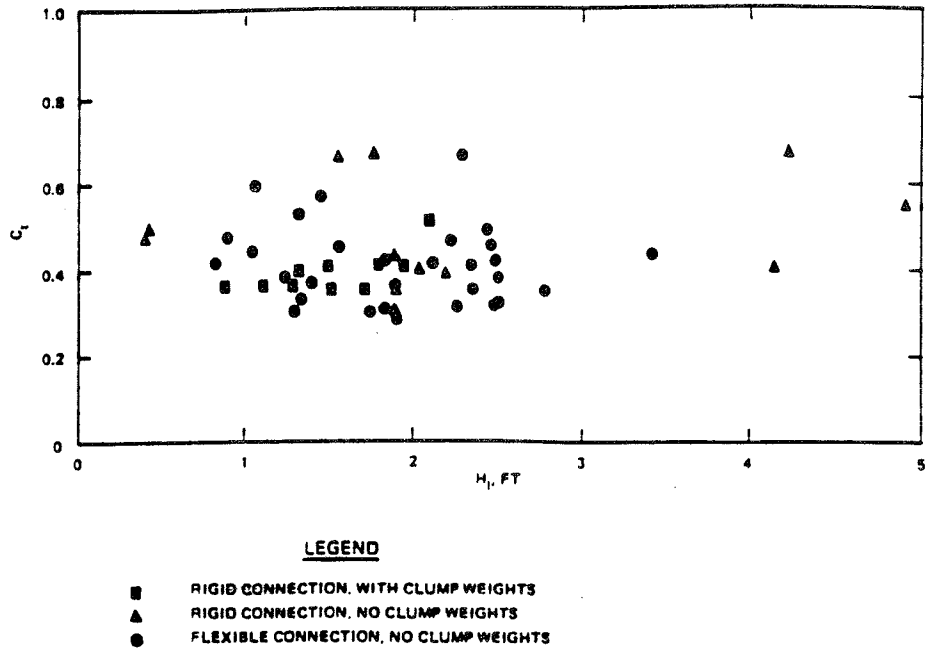

Figure 9. Transmission coefficient, Ct, versus incident wave height, Hi; concrete breakwater

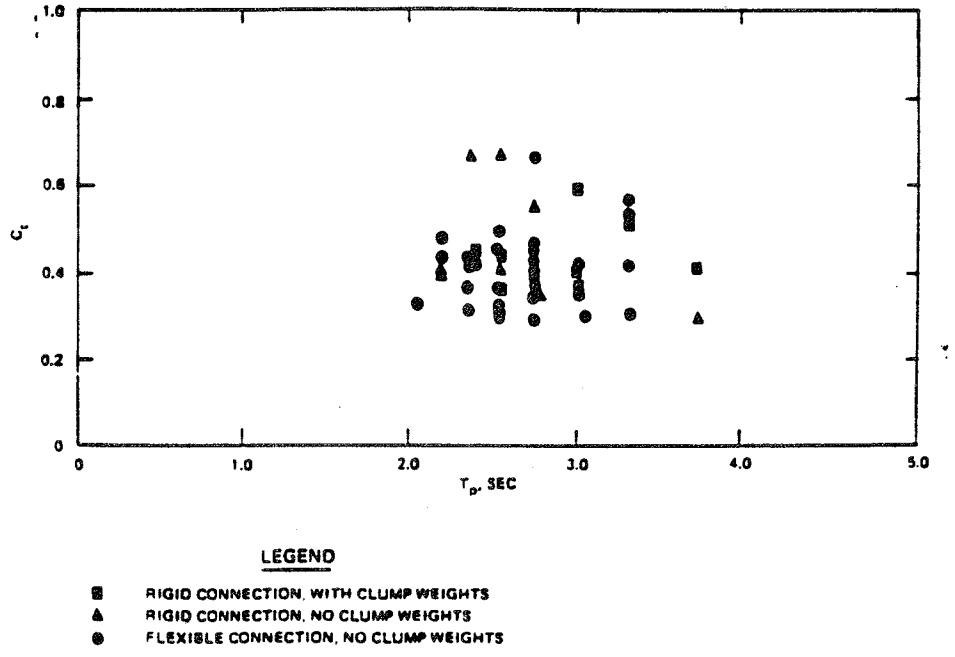

Figure 1Ø. Transmission coefficient, Ct, versus wave period, Tp; concrete breakwater

tation of more structurally oriented data collected during the FBPTP (Mlakar and Grace, 1987)(England, 1985). Parameters that were measured included hydrodynamic pressure, acceleration, relative motion, connector force, and structural strain.

12. The south face of the breakwater was equipped with 14 side-mounted pressure transducers. This instrumentation was included in an attempt to gather data relative to the effective crest lengths of waves which typically attack a floating breakwater. In many cases, methods used to predict design wave forces on a floating structure are based on the assumption that the structure is subjected to long-crested waves. Increased knowledge concerning lengths of wave crests characteristic of sites where floating breakwaters are applicable would assist in the development of more realistic and less conservative predictions of design wave forces. Previous work related to this topic was performed by Seltzer (1979) and Georgiadis and Hartz (1982). The basic assumption inherent to the analysis of this pressure data was that a continuous wave crest existed as long as a high coherency was maintained between one pressure cell and others as increasing distances between cells were considered. In other words, if a long-crested wave attacked the breakwater with its crest parallel to the structure's long axis, ideally the pressures recorded along the face of the breakwater would show high coherencies and near zero phase differences. For short-crested waves and/or for waves with angular directions of attack, the coherency between transducer readings should decrease as the distance between the transducers increases. This approach was investigated by plotting coherency between measurements as a function of distances between transducers. The results of such a plot are shown in Figure 11 which indicates that during this storm event, coherencies, as expected, decreased

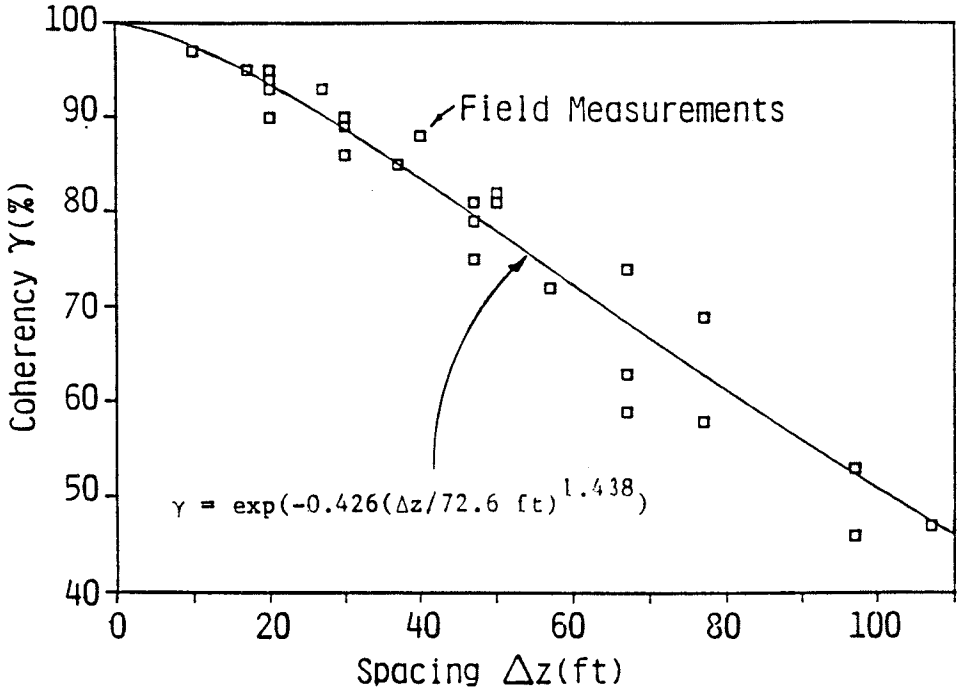

Figure 11. Spatial correlation of hydrodynamic pressures

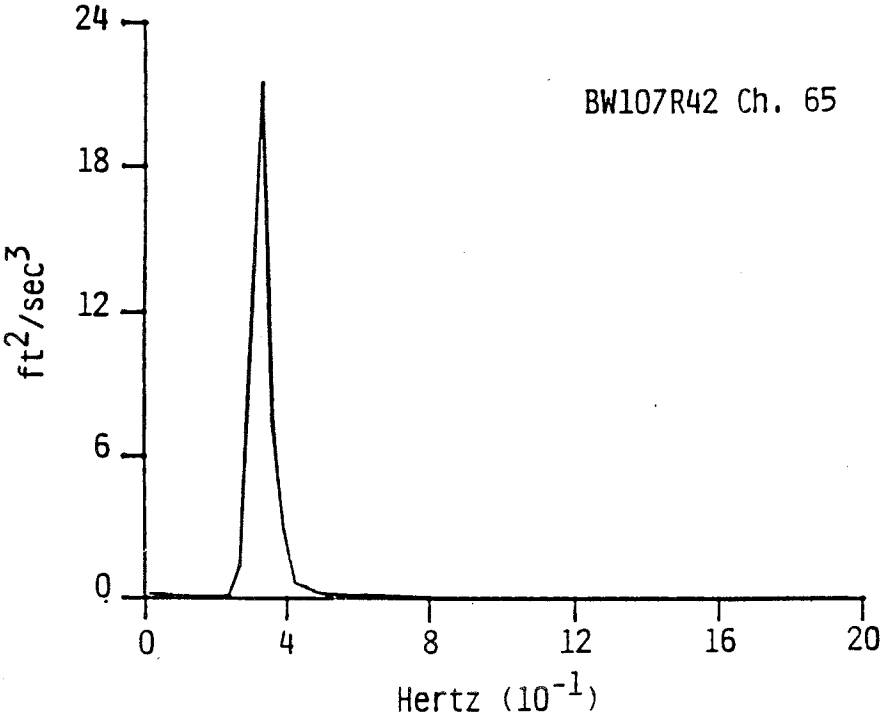

Figure 12. Sway acceleration of breakwater

as the transducer spacings increased. This data was further used in conjunction with a method to describe the spatial correlation of the wave loading presented by Georgiadis and Hartz (1982). With this method it is assumed that wave pressure coherencies along the breakwater will vary exponentially, and for two points separated by the distance Δz, the coherency, γ, will be of the form:

$$\gamma(\Delta z/\lambda) = \exp(-\alpha(\Delta z/\lambda)^{\beta}) \quad (1)$$

where λ = wavelength and α and β are characteristics of the wave directional spectrum. For the particular event presented here, λ = 72.6 ft and α and β were Ø.426 and 1.438, respectively. The resulting theoretical prediction based on this event is also shown in Figure 11. The figure indicates that the method of predicting wave pressure coherency presented by Georgiadis and Hartz (1982) produced results in good agreement with the field measured values.

Accelerations

13. Each of the two breakwater modules was equipped with one angular and two linear accelerometers. This allowed monitoring of roll, heave, and sway accelerations from each section. The autospectrum of sway acceleration for a storm record in which Hs = 2.9 ft and Tp = 3.Ø sec is shown in Figure 12. The sway motion has a standard deviation of 1.2 ft/sec. The peak response occurs at a period of 3.Ø sec which is indicative of a linear system.

14. One of the objectives for field measurement of accelerations was for their use in comparison with corresponding accelerations predicted by numerical models. An extensive analysis of a portion of the Puget Sound acceleration data was performed previously (Miller, et al.,

1984). The purpose of that study was to compare the field measured accelerations to accelerations predicted by an analytical model which estimated the six-degree-of-freedom response of a rigid body due to harmonic loadings. In general, the authors concluded that in the regions of maximum acceleration response, the rigid body response sea-keeping theory adequately predicted floating breakwater accelerations in beam seas. For the purpose of this memorandum, acceleration records were chosen and simply compared to the results of this previous analysis. In all cases, the measured results again agreed well with those estimated in terms of the natural frequencies in roll and heave. Original analysis plans included calculation of forces and moments after transformation of the acceleration data to the strain gage locations. Results of structural analysis based on strain and based on accelerations could then have been compared to each other and to numerical predictions. Failure of the data analysis system, and time and funding restraints prevented execution of those original plans.

Relative Motions

15. Relative motions between the two breakwater modules were measured during that time when the horizontal flexible connector was in place. A rotating, extendable shaft with U-joints at each end was fabricated for this purpose. The shaft incorporated a linear and rotational potentiometer to transduce the surge and roll motions, respectively. In each U-joint, rotational potentiometers measured the pitch and yaw responses. While all six relative motions between the modules can be deduced from these measurements, the pitch motions are of primary concern when evaluating the horizontal fendering connection. The

pitch between the two breakwater pontoons is the algebraic difference of the corresponding measurements at each U-joint of the relative motion device. The amplitude of the FFT of the pitch response between modules for a storm record in which Hs = 2.4 ft and Tp = 3.Ø sec is shown in Figure 13. The magnitude of the pitch response was moderate with a standard deviation of 1.2 degrees. It should be noted that the characteristic period of the pitch response, 3.Ø sec, coincides with the peak period of the storm waves, indicating a linear relationship. Further analysis of the relative motion data would allow design improvements relative to the horizontal fender connection. The data could also serve to validate methods to analytically predict characteristics of breakwater response.

Connector Loads

16. During the last two months of the monitoring effort, forces in the outer four longitudinal bolts of the horizontal fender connection were measured. To accomplish this, a Ø.15-inch diameter hole was drilled in the end of each bolt to a depth of 3 to 4 bolt diameters. A complete strain gage bridge was then mounted at the bottom of the hole using an inflatable Teflon tube and special adhesives. For a storm in which Hs = 2.5 ft and Tp = 3.Ø sec, the autospectrum of the force in the northermost bolt of the connector is shown in Figure 14. The standard deviation of this force was 1.5 kips and it is apparent that the force was characterized by a number of frequencies associated with various modes of structural response. It is reasonable to assume a linear distribution of forces in all of the bolts of the connector so that the resultant surge force and yaw moment on the connector can be estimated

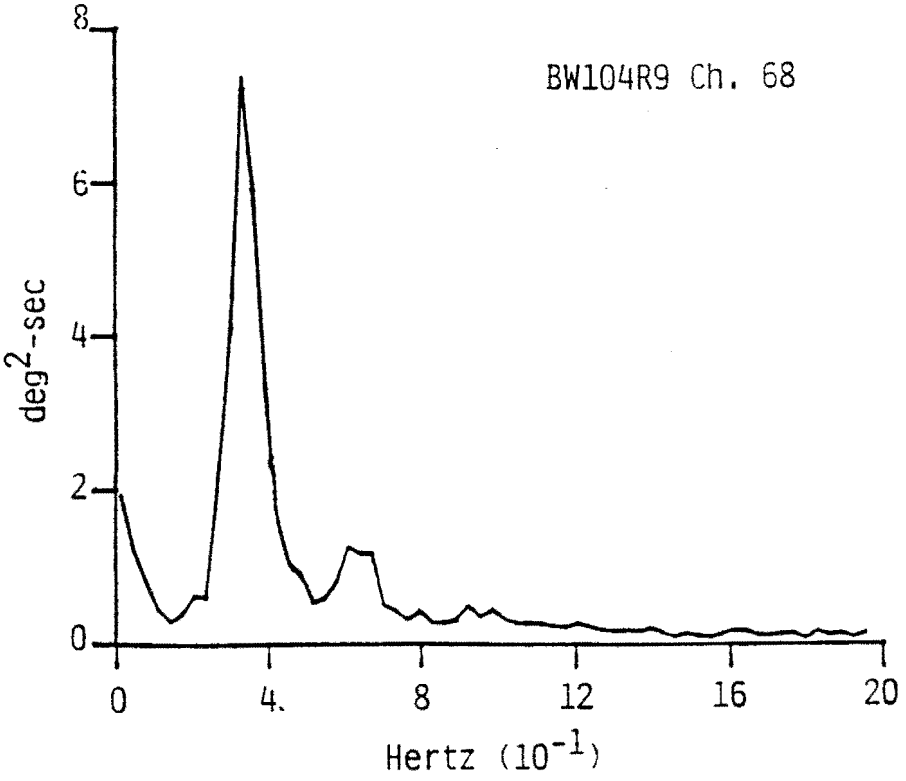

Figure 13. Pitch between breakwater modules

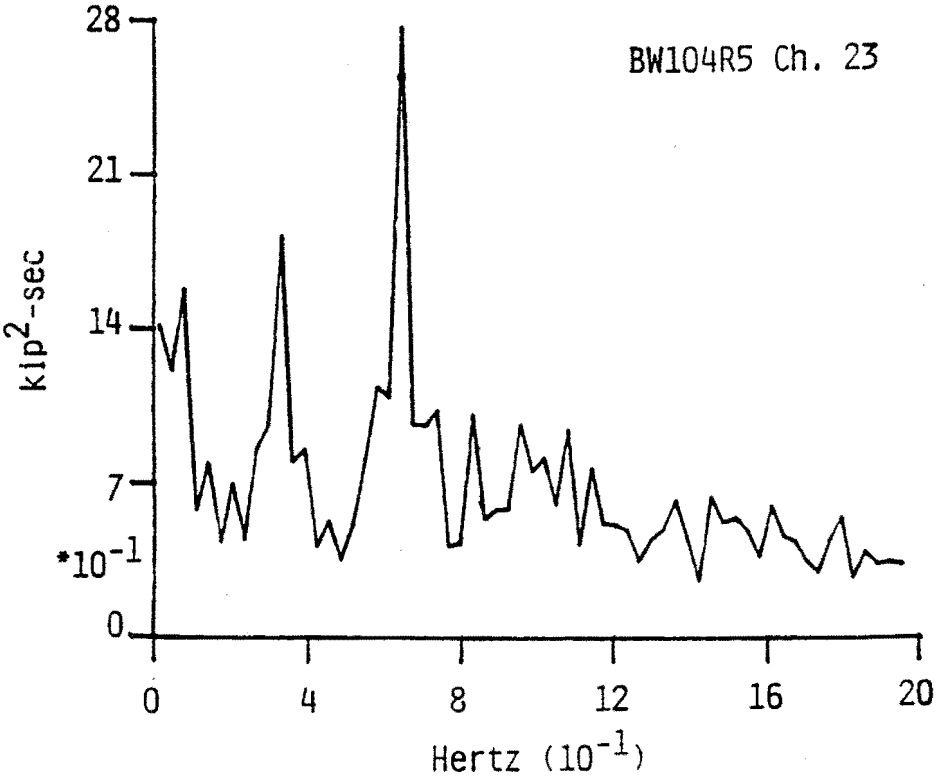

Figure 14. Force in connector bolt

from the measurements. Autospectra of these quantities for the same storm record as Figure 14 appear in Figures 15 and 16. The corresponding standard deviations were 34 kips for the surge force and 13Ø ft-kips for the yaw moment. Both resultants are dominated by a response period of 3.Ø sec.

17. Establishing a suitable flexible connecting mechanism has been the most difficult structural aspect of a floating breakwater design. The force measurements now available as a result of the FBPTP provide a more rational basis for such designs. The data permits an immediate improvement of the horizontal fender connector for the particular floating breakwater design used in the field study. The data is also available for validation of analytic models of structural dynamic response which could then be used to estimate forces typical of situations with other connecting mechanisms and/or breakwater designs.

Structural Strains

18. Internal concrete strains were measured at 12 locations within the west module. This was accomplished with complete strain gage bridge circuits bonded to 3-ft lengths of No. 5 machined reinforcing steel. The 12 measurements made included the longitudinal strains in the four corners of a cross-section at the center of the structure and in the four corners of a cross-section adjacent to the east end. Also at the latter cross-section, diagonal strains at the midpoints of the four outer walls were measured. The two cross-sections and gages associated with corner measurements of longitudinal strain, ϵ_i, are shown in Figure 17. The corresponding normal stresses, $E\epsilon_i$, are related to the axial force, P, the sway moment, My, and the heave moment, Mz, as

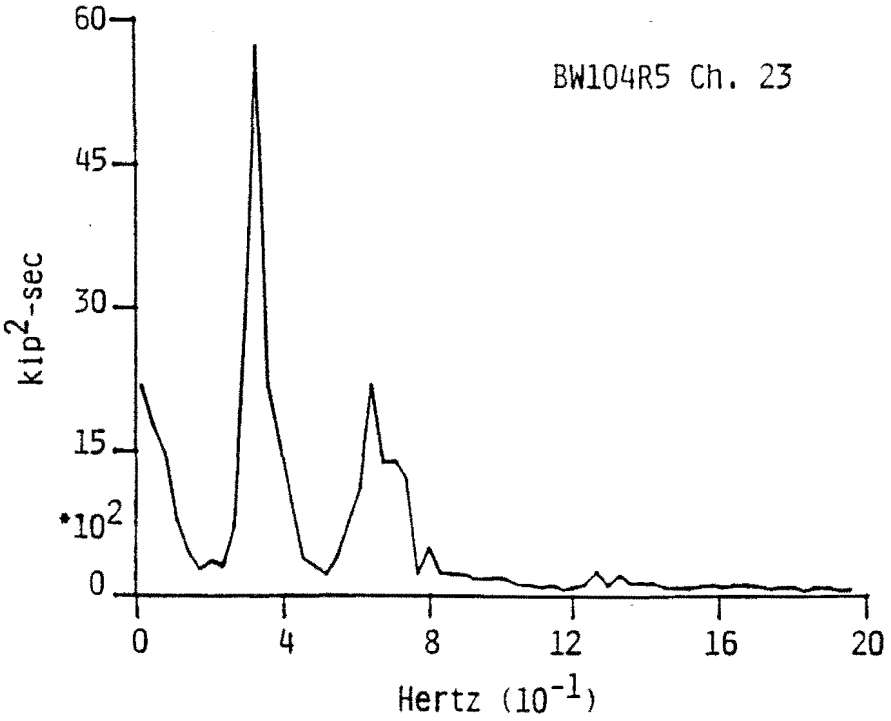

Figure 15. Resultant surge force between breakwater modules

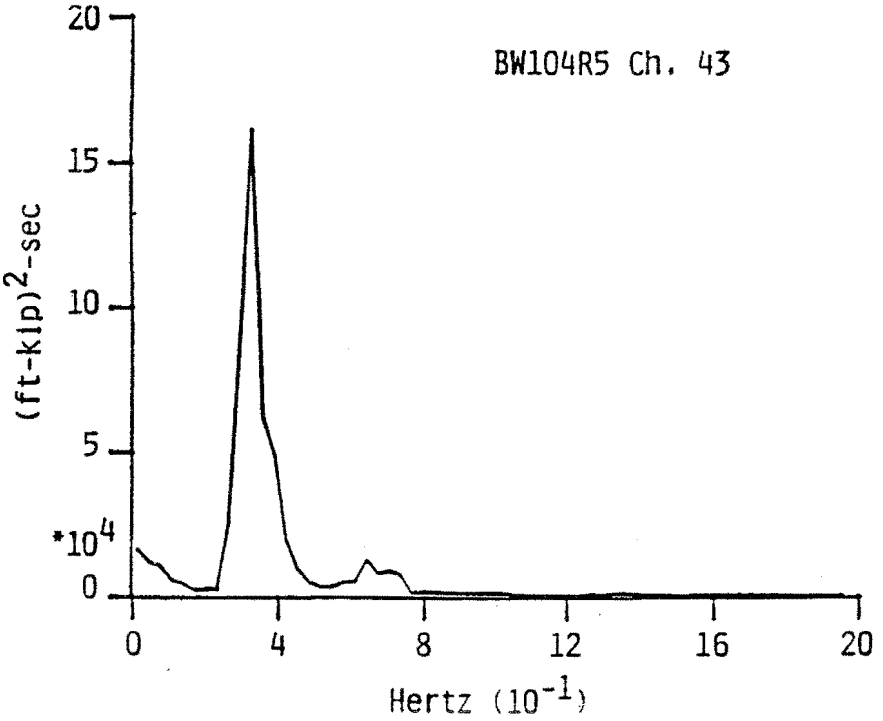

Figure 16. Resultant yaw moment between breakwater modules

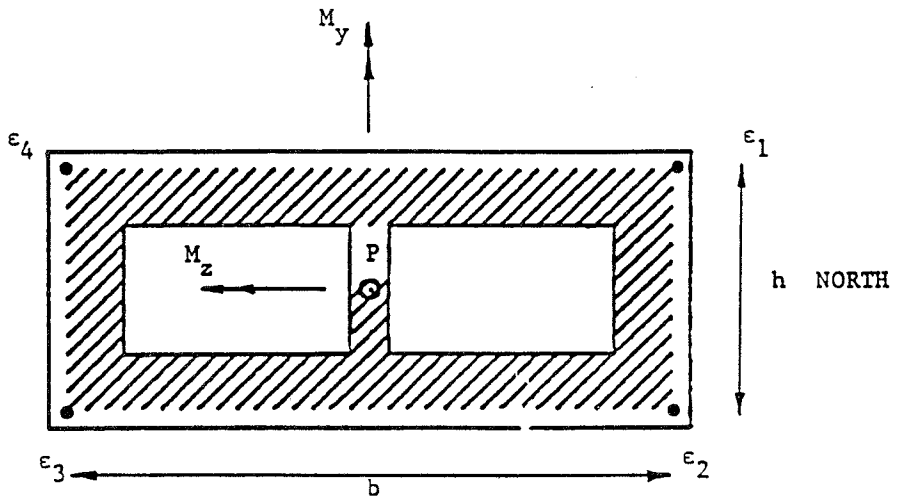

Figure 17. Typical breakwater cross-sections with longitudinal gages

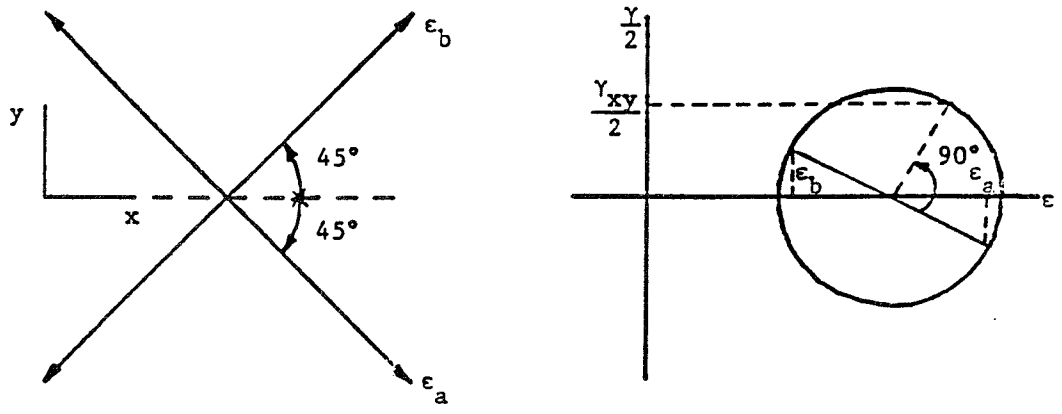

a. diagonal gage pair b. Mohr's circle

Figure 18. Diagonal strain gage information

indicated below:

$$E(\varepsilon_1) = P/A - \frac{(My)b}{2(Iy)} - \frac{(Mz)h}{2(Iz)} \quad (2)$$

$$E(\varepsilon_2) = P/A - \frac{(My)b}{2(Iy)} + \frac{(Mz)h}{2(Iz)} \quad (3)$$

$$E(\varepsilon_3) = P/A + \frac{(My)b}{2(Iy)} + \frac{(Mz)h}{2(Iz)} \quad (4)$$

$$E(\varepsilon_4) = P/A + \frac{(My)b}{2(Iy)} - \frac{(Mz)h}{2(Iz)} \quad (5)$$

where E = modulus of elasticity
A = cross-sectional area
Iy = sway moment of inertia
Iz = heave moment of inertia
b = breakwater width
h = breakwater height

Equations 2 through 5 overdetermine the three unknown force resultants. It is rational to estimate them by minimizing the sum of the squared differences between measured and theoretical stresses, i.e.:

$$\min_{P,My,Mz} \left[\left(E\varepsilon_1 - \frac{P}{A} + \frac{(My)b}{2(Iy)} + \frac{(Mz)h}{2(Iz)} \right)^2 + \ldots + \left(E\varepsilon_4 - \frac{P}{A} - \frac{(My)b}{2(Iy)} + \frac{(Mz)h}{2(Iz)} \right)^2 \right]$$

The results of equating to zero the partial derivatives of this expression with respect to each force resultant are:

$$P = \frac{EA}{4} (\varepsilon_1 + \varepsilon_2 + \varepsilon_3 + \varepsilon_4) \quad (6)$$

$$My = \frac{E(Iy)}{2b} (\varepsilon_3 + \varepsilon_4 - \varepsilon_1 - \varepsilon_2) \quad (7)$$

$$Mz = \frac{E(Iz)}{2h} (\varepsilon_2 + \varepsilon_3 - \varepsilon_1 - \varepsilon_4) \quad (8)$$

Equations 6 through 8 constitute the desired transformations between longitudinal strains and force resultants. For the actual prototype

data, values of i=1 through i=4 correspond to measurements from channels 45 through 48, and channels 57 through 60, from the two cross-sections equipped with longitudinal strain gages.

19. As mentioned previously, one cross-section of the breakwater contained four pairs of diagonal strain gages. This instrumentation was included to measure shear strains at those four locations. The orientation of a gage pair, ε_a and ε_b, on the vertical side walls is shown in Figure 18. From the corresponding Mohr's circle for strain, it follows that the shearing strain on the plane of the cross-section is:

$$\gamma_{xy} = \varepsilon_a - \varepsilon_b \tag{9}$$

For the measured prototype data, it follows that:

$$\gamma_1 = \varepsilon_{49} - \varepsilon_{50} \tag{10}$$

$$\gamma_2 = \varepsilon_{52} - \varepsilon_{51} \tag{11}$$

$$\gamma_3 = \varepsilon_{54} - \varepsilon_{53} \tag{12}$$

$$\gamma_4 = \varepsilon_{55} - \varepsilon_{56} \tag{13}$$

where the values of γ_i originate from the locations shown in Figure 19. Those shearing strains were measured to estimate the torque, T, sway shear, Vy, and heave shear, Vz, acting on that cross-section. These quantities are related as follows:

$$G(\gamma_1) = \frac{bT}{2J} + \frac{Vy}{h(2t + t')} \tag{14}$$

$$G(\gamma_2) = \frac{hT}{2J} + \frac{Vz}{2bt + ht'} \tag{15}$$

$$G(\gamma_3) = \frac{hT}{2J} + \frac{Vz}{2bt + ht'} \tag{16}$$

$$G(\gamma_4) = \frac{bT}{2J} + \frac{Vy}{h(2t + t')} \tag{17}$$

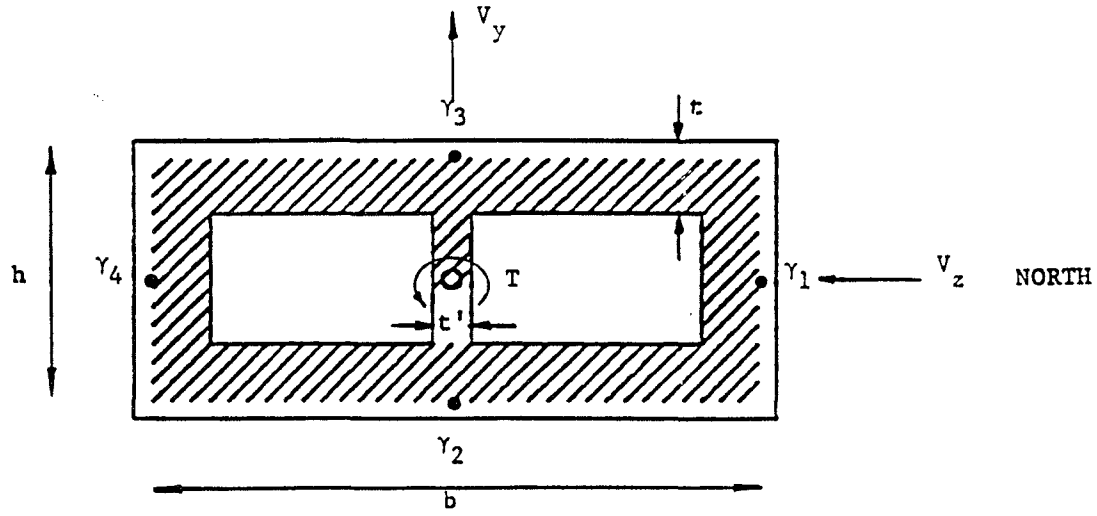

Figure 19. Breakwater cross-section with diagonal gages

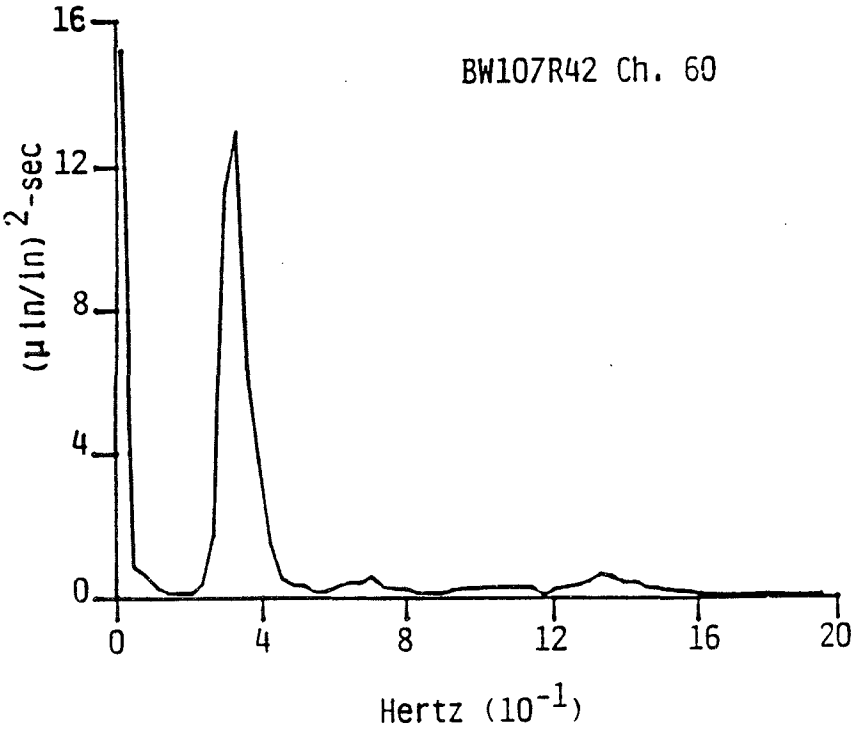

Figure 2Ø. Longitudinal strain in lower south corner at center of west pontoon

where G = shear modulus
J = polar moment of inertia
t = outer wall thickness
t′ = inner wall thickness

The force resultants are estimated by minimizing the sum of the squared differences between measured and predicted shearing stress, i.e.:

$$\min_{T,Vy,Vz} \left[\left(G(\gamma_1) - \frac{b}{2J} - \frac{Vy}{h(2t + t')} \right)^2 + \ldots + \left(G(\gamma_4) + \frac{b}{2J} T - \frac{Vy}{h(2t + t')} \right)^2 \right]$$

The resulting equations are:

$$T = JG \frac{b(\gamma_1 - \gamma_4) + h(\gamma_3 - \gamma_2)}{b^2 + h^2} \tag{18}$$

$$Vy = h(2t + t')G \frac{\gamma_1 + \gamma_4}{2} \tag{19}$$

$$Vz = (2bt + ht')G \frac{\gamma_2 + \gamma_3}{2} \tag{20}$$

Therefore, the required transformations between diagonal strain data and internal force resultants are established in equations 10 through 13 and equations 18, 19, and 20.

20. The autospectrum of longitudinal strain in the lower south corner, center cross-section, of the west pontoon is shown in Figure 20. These strains were measured during a storm event characterized by an Hs = 2.9 ft and Tp = 3.0 sec. Aside from the zero frequency component, the peak strain occurred at a period of 3.0 sec which again coincides with the wave period. The standard deviation of this strain is only 1.5 in/in, a strain magnitude of no consequence to the integrity of the structure; however, the surge force, yaw moment, and pitch moment for each cross-section can also be estimated from the arrangement of the four longitudinal gages using prismatic beam theory. The pitch bending moment so obtained which corresponds to Figure 20 is shown in

Figure 21. This resultant has a standard deviation of 68 ft-kips with maximum response at a period of 3.Ø sec. An energy density plot of sway shear force (corresponding to the same storm) is shown in Figure 22. The standard deviation and the peak period of this resultant are 18 kips and 3.Ø sec, respectively. Note again that the periods at which peak force resultants occur coincide with the period of peak wave energy, indicating a linear response.

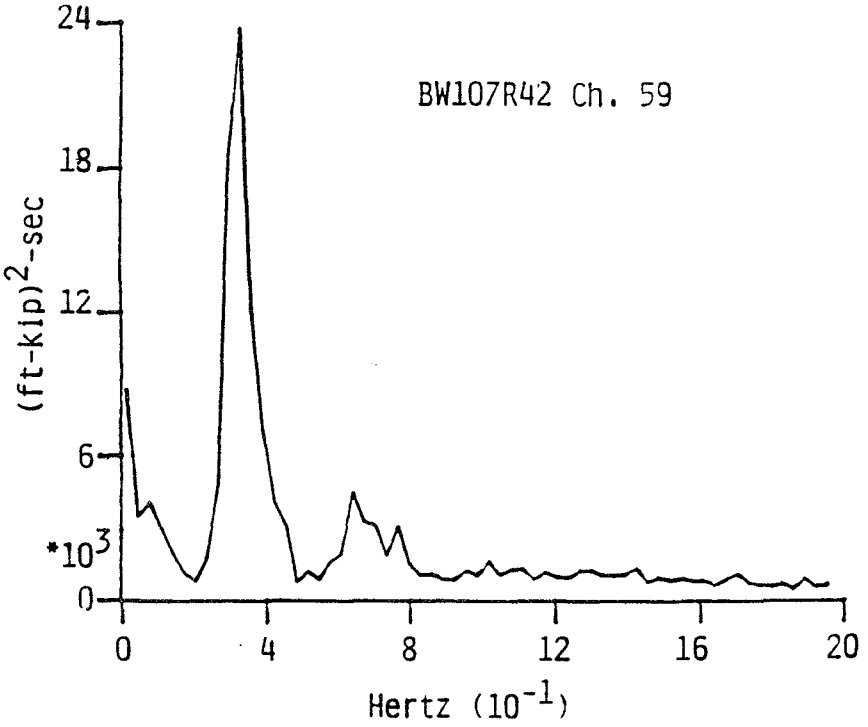

Figure 21. Pitch bending moment at center of west pontoon

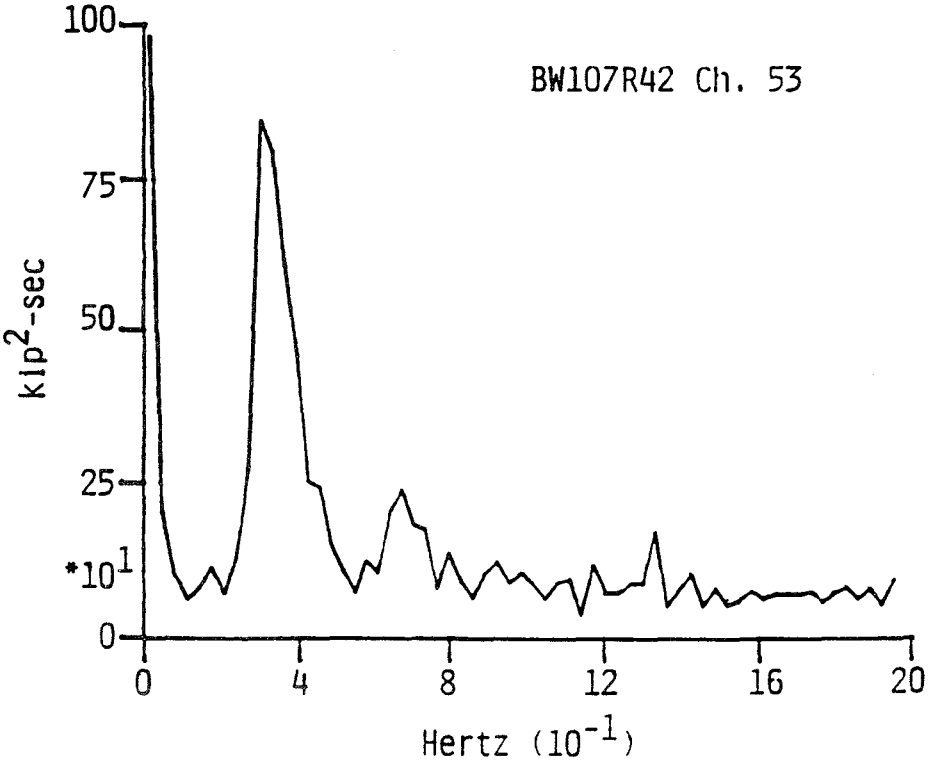

Figure 22. Sway shear force in west pontoon

PART IV: CONCLUSIONS

21. Based on the results of data analysis efforts completed to date, the following conclusions have been made:

a) For wave periods of four seconds and less, current methods of predicting wave transmission by floating breakwaters are adequate.

b) Measured anchor line forces were substantially lower than predicted loads, i.e. load predictions based on linear theory and physical model tests. Design of mooring systems may be primarily influenced by factors such as corrosion or berthing loads rather than wave induced tensile loads in the lines.

c) Forces at the connection of the mooring line to the breakwater were approximately 25% greater than corresponding forces at the connection to the anchor pile.

d) Removal of clump weights from the anchor lines resulted in an increase in the upper anchor line load while loads in the lower load cell decreased.

e) The response of the prototype breakwater was dominated by rigid body motion and magnitudes of measured strains were in all cases very small. Maximum stresses were experienced during the process of lifting and launching the structure from the dry dock on which it was constructed.

f. Heave moments calculated based on the measured strain data were less than moments predicted by FLOATX. England (1985) reported that in all cases except for torsion, FLOATX predictions were conservative and floating structures could be designed with confidence using FLOATX. His results showed that if input conditions included the significant wave height used in the original breakwater design, FLOATX predictions would suggest that the structure had been overdesigned by a factor of 4.

g. Breakwater wall thicknesses should be determined by minimum reinforcement cover as specified by building requirements of the American Concrete Institute.

h. Results indicate that the prototype anchoring system was substantially overdesigned. Establishment of design mooring forces should be based on consideration of wave induced tensile forces in the mooring lines, spacings between adjacent lines, materials used in the anchoring system, corrosion susceptibility, breakwater motions, possibility of added mass due to berthed vessels, impact loads, and other possible loading parameters. Efforts have been ongoing to develop numerical mooring load prediction techniques which would allow a designer to vary the above anchor system characteristics, breakwater characteristics, and input wind and wave conditions, and evaluate

the effect on resulting anchor line loads. A frequency domain model was procured, modified, and evaluated through comparison with prototype data (Bando and Sonu, 1987). Although results compared relatively well, the method is very dependent on a user given stiffness coefficient which, in itself, is difficult to establish. In addition to this model, the Alaska District has been developing a time domain analysis mooring force prediction technique over the past few years. Documentation of their efforts should be available in FY 1989.

REFERENCES

Bando, K., and Sonu, C.J. 1988. "Development and Verification of Numerical Models for Floating Breakwaters," Contract Report CERC-88- (in publication), U.S. Army Engineer Waterways Experiment Station, Vicksburg, MS.

Bishop, C.T. 1984. "Field Assessment of Floating Tire Breakwater," National Water Research Institute, Burlington, Ontario, Canada.

Christensen, D.R. 1984. "Installation, Operation, and Maintenance Manual for Breakwater Data Acquisition System," Water Resources Series Technical Report No. 91, Department of Civil Engineering, University of Washington, Seattle, WA.

England, G.C. 1985. "Testing and Analysis of a Floating Breakwater," Masters Thesis, Structural and Geotechnical Engineering and Mechanics Program, Department of Civil Engineering, University of Washington, Seattle, WA.

Georgiadis, C., and Hartz, B.J. 1982. "A Computer Program for the Dynamic Analysis of Continuous Floating Structures in Short Crested Waves," C.W. Harris Hydraulics Laboratory Technical Report No. 74, Department of Civil Engineering, University of Washington, Seattle, WA.

Grace, P.J., and Clausner, J.E. 1987. "Floating Tire Breakwater Tests Pickering Beach, Delaware," Miscellaneous Paper CERC-87-21, U.S. Army Engineer Waterways Experiment Station, Vicksburg, MS.

Miller, R.W., Christensen, D.R., Nece, R.E., and Hartz, B.J. 1984. "Rigid Body Motion of a Floating Breakwater: Seakeeping Predictions and Field Measurements," Water Resources Series Technical Report No. 84, Department of Civil Engineering, University of Washington, Seattle, WA.

Mlakar, P.F., and Grace, P.J. 1987. "Prototype Floating Breakwater Structural Test Data," ASCE Proceedings: Computer Aided Simulation of Fluid-Structure Interaction Problems, American Society of Civil Engineers, New York, NY.

Nelson, E.E., and Broderick, L.L. 1986. "Floating Breakwater Prototype Test Program: Seattle, Washington," Miscellaneous Paper CERC-86-3, U.S. Army Engineer Waterways Experiment Station, Vicksburg, MS.

Seltzer, G.H. 1979. "Wave Crests - How Long?" Masters Thesis, University of Washington, Seattle, WA.